PWCs AND DRIFT CHAMBERS AT ISABELLE **

H. Okuno,* BNL
Y. Teramoto,† BNL
C.D. Wheeler, BNL
A.H. Walenta, BNL
S.J. Lindenbaum, BNL & ~~CUNY~~
H.B. Jensen,‡ CERN
B. Sadoulet, CERN
M. Atac, Fermilab
R. Stump, University of Kansas
A. Kanofsky, Lehigh University
R. Weinstein, Northeastern University
S. White, Rockefeller University

At the 1977 Workshop, attempts were made to predict the behavior of proportional wire chambers at the high particle flux expected for ISABELLE.[1] It was found that chambers running at the now widely used high gas gain would have impaired performance with regard to lifetime, efficiency, stability of gas gain, and position resolution. More information has since become available, and therefore the predictions about these properties are revised in the present study.

Improvement can also be expected with much lower gas gain, a possibility that is investigated here in more detail with regard to its effect on position resolution and time resolution.

The expected high multiplicity of tracks from a single event, the high event rates, and the requirement for low gas gain necessitate revision of the methods for measuring the second coordinate.

Particle identification via measurement of the relativistic rise of energy loss in the chambers has been investigated in more detail than previously, with new data and calculations.

RATE EFFECTS IN PROPORTIONAL CHAMBERS AND DRIFT CHAMBERS

The high particle rates expected at ISABELLE raise fundamental questions about the operation of proportional and drift chambers, as discussed, e.g., by Walenta[1] in 1977. Here we summarize results on the chamber lifetime based on new measurements and more detailed considerations of space-charge effects and gain saturation.

Particle Rates

Charged particle rates can be estimated according to calculations made by Paige.[2] A simple approximation to the cross section curve $\sqrt{s}$ = 800 GeV gives

$$d\sigma/d\Omega \approx 8\times10^{-27}/\theta^{1.9} \quad (cm^2\ sr^{-1}) \qquad \text{for } 10^{-3} \le \theta \le 0.5\ ,$$

$$d\sigma/d\Omega \approx 13\times10^{-27}/\theta^{1.2} \quad (cm^2\ sr^{-1}) \qquad \text{for } 0.5 \le \theta \le \pi/2\ . \quad (1)$$

*On leave from Institute for Nuclear Study, University of Tokyo.

†On leave from Osaka City University.

‡On leave from Niels Bohr Institute, Copenhagen.

**Supported in part by the United States Department of Energy.

For a luminosity L, the particle rate in solid angle $\Delta\Omega$ is given by

$$\text{rate} = L\frac{d\sigma}{d\Omega}\Delta\Omega \quad (\text{particles } s^{-1}) \quad . \tag{2}$$

The particle rate per unit wire length of the chamber depends on the configuration and geometries of the chamber. Typical examples are shown in Fig. 1, where the scattering angle θ is divided into three regions.

Region I ($30^\circ \leq \theta \leq 150^\circ$) is covered by a "bicycle-wheel" drift chamber, which is segmented into N sections. The particle rate per unit wire length (1 cm) is[3]

$$n = L\frac{d\sigma}{d\Omega}\frac{1}{r}\frac{2\pi}{N}\sin^3\theta \quad (\text{particles cm}^{-1}\ s^{-1}) \quad . \tag{3}$$

The lifetime of the chamber and space-charge effects are considered to depend on the product of the n mber of particles and the size of the avalanche. If the size of the avalanche for the particle track perpendicular to the anode wire is q_o, then the avalanche size for the inclined track is $q = q_o/\sin\theta$. Then the charge rate Q per unit wire length is

$$Q = nq = L\frac{d\sigma}{d\Omega}\frac{1}{r}\frac{2\pi}{N}\sin^2\theta\ q_o \quad (\text{electrons cm}^{-1}\ s^{-1}) \quad . \tag{4}$$

Q along the anode wire changes only by a factor of 2 in this region, and is almost constant at small θ because of Eq. (1). The maximum Q is at $\theta = 30^\circ$, and for $L = 5\times10^{32}$ cm^{-2} s^{-1} (the expected luminosity in the low-β configuration),

$$Q_{max} = 2.2\times10^7 q_o/rN \quad (\text{electrons cm}^{-1}\ s^{-1}) \quad . \tag{5}$$

In order to get the optimum value of Q_{max}, we can adjust three parameters: r, N, and q_o. For r = 10 cm, N = 90, and $q_o = 2\times10^6$ e, $Q_{max} = 4.8\times10^{10}$ e cm^{-1} s^{-1}, and the rate per wire is about 10^6 particles s^{-1}.

Since the particle rate increases at smaller angles, region II ($10^\circ \leq \theta \leq 30^\circ$) is covered by circular, flat drift chambers with relatively narrow drift space. With drift space d, the particle rate per unit length of wire is

$$n = L\frac{d\sigma}{d\Omega}\frac{d}{r^2}\sin^2\theta\cos\theta \quad (\text{particles cm}^{-1}\ s^{-1}) \quad . \tag{6}$$

At $\theta = 10^\circ$ and $L = 5\times10^{32}$ cm^{-2} s^{-1},

$$Q_{max} = 3.2\times10^6(d/r^2)q_o \quad (\text{electrons cm}^{-1}\ s^{-1}) \quad . \tag{7}$$

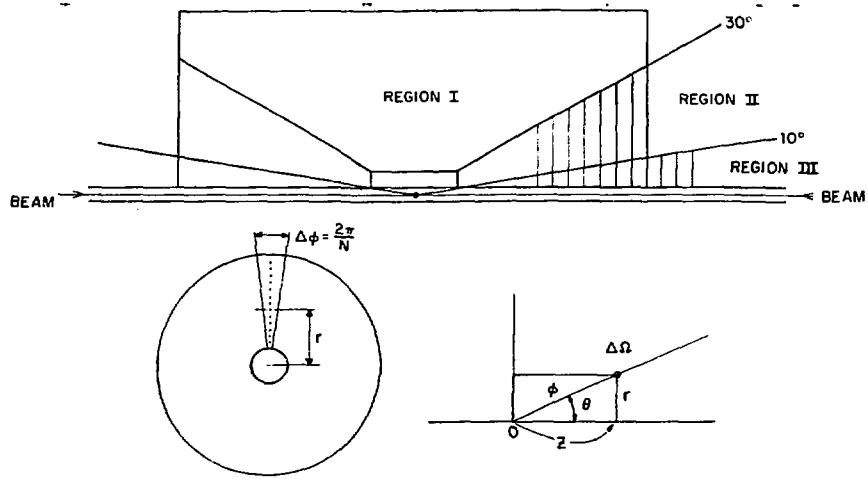

Fig. 1. Chamber arrangement around an intersection region.

For r = 10 cm, d = 0.5 cm, and $q_o = 2\times10^6$ e, $Q_{max} = 3.2\times10^{10}$ e cm^{-1} s^{-1}.

In region III ($\theta \leq 10^o$), $d\sigma/d\Omega$ is roughly proportional to $1/\theta^2$, and $\sin^2\theta \cos\theta = \theta^2$. Therefore, particle rate is simply expressed (see also Etkin[4]), as

$$n = 3.2\times10^6 d/r^2 \quad (\text{particles } cm^{-1}\ s^{-1}). \qquad (8)$$

For r = 3 cm, d = 0.2 cm, and $q_o = 2\times10^6$ e, one obtains $n = 7\times10^4$ particles cm^{-1} s^{-1} and $Q_{max} = 1.4\times10^{11}$ e cm^{-1} s^{-1}. When chambers are placed at z = 500 cm, the minimum angle covered is $\theta = 0.006$.

Lifetime

The lifetime of the chamber is limited because of the polymerizing effect of some quenchers or impurities. Long exposure to intense radiation causes formation, on the anode and the cathode, of polymer deposits, which result in decreased gas gain, deterioration of energy resolution, and increased background.

Accumulation of a critical amount of deposits is, in simple approximation, considered to be proportional to the integral amount of free charges created in the avalanche per unit wire length. The definition of a critical value, Q_{crit}, for deterioration of the chamber depends on the operation mode of the chamber. When the chamber is used for dE/dx measurement, gain variations of a few percent cause problems, but when it is used only for position readout, the requirement for energy resolution is less stringent.

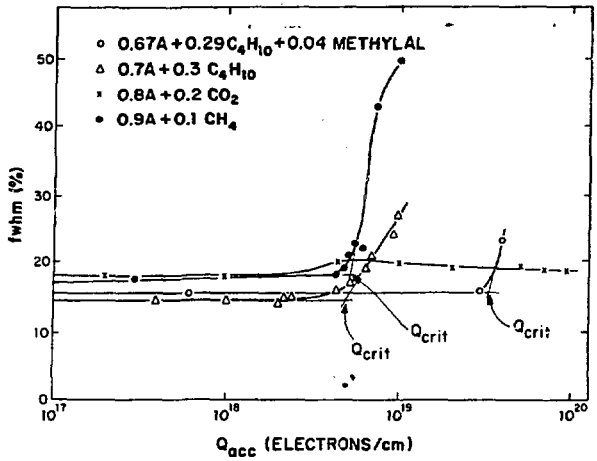

Fig. 2. Energy resolution of a proportional counter for ^{55}Fe over total accumulated charge per wire length.

In 1977, Q_{crit} was estimated to be 2.5×10^{17} e cm^{-1} on the basis of Geiger counter data. To check the validity of this estimate, new measurements were made at BNL.[5] Preliminary results are shown in Fig. 2, where the energy resolution for ^{55}Fe x rays (5.9 keV) is plotted as a function of the accumulated free charge. If we define Q_{crit} as the integrated charge where the energy resolution varies as shown in Fig. 2, Q_{crit} for various gas mixtures can be compared as shown below:

	Q_{crit} (e cm^{-1})
Ar (90%) + CH_4 (10%)	5.3×10^{18}
Ar (70%) + isobutane (30%)	5.4×10^{18}
Ar (67.2%) + isobutane (28.8%) + methylal (4%)	3.3×10^{19}
Ar (80%) + CO_2 (20%)	$>10^{20}$

The best result is obtained for the Ar-CO_2 mixture. This mixture may be considered if necessary, but further investigation of its behavior in drift chambers is needed. For Ar-isobutane, addition of a small amount of methylal lengthens the counter life appreciably.

By using the Q_{crit} value for Ar-isobutane-methylal, the lifetimes of the chambers described in the previous section can be estimated. The results (Table 1) are encouraging. Note, however, that the assumed value of Q_{crit} was obtained with a small cylindrical test tube and with the clean gas system, and further studies should be made on the effects of wire cathodes and of impurities.

Table 1

Lifetime of Chambers

$L = 5 \times 10^{32}$ cm^{-1} s^{-1}, $q_o = 2 \times 10^6$ e, and

$Q_{crit} = 3 \times 10^{19}$ e cm^{-1} are assumed

	Type of chamber	r_{min} (cm)	Max particle rate, n_{max} (10^4 cm^{-1} s^{-1})	$Q_{max} = nq_o$ (10^{10} e cm^{-1} s^{-1})	Life-time (yr)
Region I	Bicyle-wheel drift chamber N = 90	10	2.4	4.8	20
Region II	Circular, flat drift chamber d = 0.5 cm	10	1.6	3.2	30
Region III	PWC d = 0.2 cm	3	7.0	14.0	7

Space-Charge Effect

In dE/dx measurements for particle identification, the gain shift of the chamber due to the space charge of positive ions is a serious problem at high rates. With a typical geometry of the drift chamber (d = 1 cm), 2% gain shift was observed[1] at $Q = 5 \times 10^{10}$ e cm^{-1} s^{-1}. Recent results at CERN[6] also showed a gain shift of about 2% at $Q = 10^{10}$ e cm^{-1} s^{-1} for the drift chamber of d = 2 cm. These numbers are compatible with Q_{max} for each configuration of chambers given in Table 1. In regions II and III, smaller drift distances are chosen, so that the space-charge effect will be much reduced. Therefore, chamber geometries considered in Table 1 seem to be acceptable.

When a relatively long drift space is required, a possible means of reducing the space-charge effect is the introduction of grid wires near the anode wire. In Fig. 3, two examples are shown. A grid has a twofold effect: (1) it reduces the number of positive ions reaching the long drift region, and (2) for positive ions escaped to the drift region, its shielding effect reduces their influence on the field near the anode. The fraction of positive ions escaping to the drift region depends on two factors: the field shape near the grid, and the azimuthal spread of positive ions

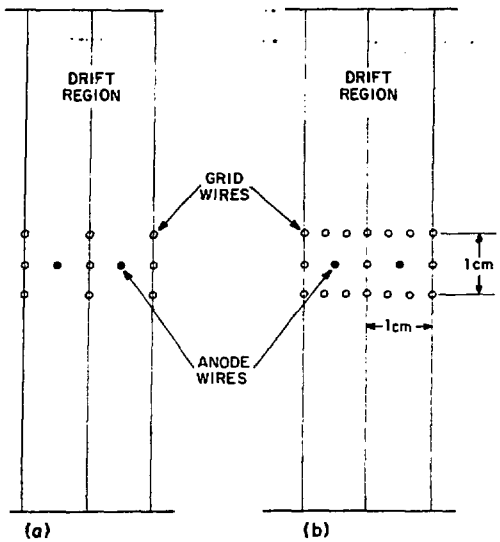

Fig. 3. Configurations of grid wires.

around the anode wire. The latter is about 100° (FWHM) in the proportional region of gas amplification for Ar (90%) + CH_4 (10%), and changes slightly depending on the amount of quencher.[7] As the avalanche is relatively well localized on one side of the wire, grid spacing should be relatively narrow compared with the grid-anode distance. By choosing a suitable potential, one can get the fraction escaping to be 0.1 to 0.5. The TPC group[8] measured a value of <0.1 for the geometry given in Fig. 3(b). For the grid planes placed 5 mm from the anode plane, a rate behavior equivalent to that of the drift chamber with d = 1 cm can be expected.

Another new approach to overcoming high rate limitations was proposed recently by G. Charpak et al.[9] which uses a preamplification zone, a drift delay, a gate (chamber requires a trigger), and a final amplification zone. The space-charge effect in the final amplification zone is reduced if the number of selected events is much smaller than the overall particle flux, but it is not yet clear how the preamplification zone behaves at high rates. Although it makes the construction of the chamber more complex, this scheme may be applied to the extremely high rate at small angles.

Gain Saturation

For dE/dx measurements, the chamber must be operated strictly in the proportional region. For better spatial resolution, a bigger avalanche size is preferable. Therefore, the maximum avalanche size in the proportional region should be chosen for actual experimental conditions. For ^{55}Fe x rays, the deviation

from linearity is about 5% at $q_o \approx (2 \text{ to } 3)\times10^6$ e. This gain saturation can be explained by the local distortion of electric field around the avalanche due to the local space charge. For typical chambers, the field on the surface of the anode is 2×10^5 V/cm. On the other hand, the field on the surface of the sphere of positive ion space charges q_o is $E_r \approx 1.7\times10^{-7} q_o/r_D^2$ (V/cm), where r_D is the radius of the positive ion cloud. The value of r_D is determined by such factors as the distribution of primary ionization diffusion of drifting electrons and avalanche spread near the anode wire. For ^{55}Fe x rays, the main contribution is the track length of emitted electrons, and r_D is about 150 μm. Then a field distortion of 1% is obtained at $q_o = 2.7\times10^6$ e, which corresponds to a gain variation up to 5%.

For charged particles crossing the chamber, this local space-charge effect depends strongly on the position and angle of the particle path with respect to the anode wire. The worst case occurs when particles cross the chamber at the position of the anode wire with an angle of 90° and leave an ionization chain that drifts toward the same spot on the anode wire. The avalanche due to the electrons arriving first may produce a space charge and reduce the original multiplication field. For simplicity, we assume that half of the primary electrons in a 5-mm gap contribute to building up the space charge. Other electrons arrive after 60 ns. At this moment, positive ions move away about 90 μm from the anode wire. Therefore, the diameter of the positive ion cloud r_D is ~100 μm. One percent distortion of the field is obtained at $q_o = 1.2\times10^6$ e, and the total avalanche size would be $q_o = 4.8\times10^6$ e because ionizations on both sides of the gap are collected on the same anode. These values are in reasonable agreement with observations in real chambers. In most experiments proposed for ISABELLE, the tracks are naturally inclined with respect to the anode wire, and therefore the proportional region would be extended.

The value $q_o = 2\times10^6$ e assumed in the previous sections seems to be reasonable as an optimum both for accurate position readout and for accurate dE/dx measurement.

Radiation Hardness of Electronics

Since some of the chamber electronics is also placed in the high radiation environment, radiation hardness of the ICs is an important factor in the lifetime of the detector system. Bipolar electronics can accept up to 10^6 rad, where the β-value shifts by 5%. Commercial CMOS can accept 10^4 rad, and 10^5 rad is possible by moderate hardening. Further improvement is possible up to 2×10^6 rad) at much higher cost. One rad is estimated to be equivalent to 3×10^7 minimum ionizing particles cm^{-2}, and the corresponding number for 10^5 rad is 3×10^{12} particles cm^{-2}. At r = 10 cm, the particle rate is about 3×10^4 cm^{-2} s^{-1}, and the expected lifetime is about 3 years. This value is somewhat lower than the chamber lifetime, but most of the electrorics can be placed relatively far from the beam axis.

In conclusion, one can choose suitable configurations of chamber geometries, and proportional and drift chambers can be used for accurate particle tracking at ISABELLE with $L = 5 \times 10^{32}$ cm^{-2} s^{-1}. Chambers can be operated at a reasonable avalanche size of $q = 2 \times 10^{6}$ e; thus both the spatial resolution, as shown below, and the energy resolution will be kept at an acceptable level.

H.B.J., H.O., A.H.W.

RESOLUTION OF DRIFT CHAMBERS

Time Resolution

The major considerations in the resolution of drift chambers are (1) the time resolution of the electronic readout system, (2) statistical fluctuations in the production of the primary ionization along a particle's path, and (3) electron diffusion during the drift time.

Because of the high rates expected at ISABELLE, it is essential to operate the chambers at the lowest possible gas gain. The resolution of drift chambers is discussed in this connection. The electronics time resolution is determined by the equivalent noise charge $(\overline{ENC^2})^{\frac{1}{2}}$ and the slope of the leading edge of the signal ds/dt:

$$\delta t = \frac{(\overline{ENC^2})^{\frac{1}{2}}}{ds/dt} \quad . \tag{9}$$

The noise depends on detector parameters such as input capacity C_{in}, resistance R_p parallel to the input, the type of amplifier, and the characteristics of the pulse-shaping circuit.

The total noise is mainly the quadratic sum of two terms, the series equivalent noise charge $(\overline{ENC_s^2})^{\frac{1}{2}}$ and the parallel equivalent noise charge $(\overline{ENC_p^2})^{\frac{1}{2}}$ (see Radeka[10] for more details):

$$\overline{ENC_s^2} = \frac{1}{2} a_{Fl} \frac{e_n^2 C_{in}^2}{t_r} \tag{10}$$

where e_n = r.m.s. equiv. series noise voltage per $Hz^{\frac{1}{2}}$, a_{Fl} = filter form factor, and t_r = signal rise time after filter;

$$\overline{ENC_p^2} = \frac{4}{3} kT \frac{t_m}{R_p} \tag{11}$$

where R_p = parallel noise resistance.

The clipping time t_m will be, for the purpose of time measurement, of the order of the fast rise time of the signal: $t_m = t_r$ = 25 ns. For a fall time of the signal $t_f = 5t_r$ one obtains $a_{Fl} = 1.2$.

Three cases will be compared, with the amplifier connected to a single anode wire so that C_{in} = 25 pF (Table 2): (1) charge-

Table 2

Equivalent Noise Charges (Electrons)

	R_p (Ω)	$(\overline{ENC_p^2})^{\frac{1}{2}}$	$(\overline{ENC_s^2})^{\frac{1}{2}}$	$(\overline{ENC_{tot}^2})^{\frac{1}{2}}$	δt (ns)
Charge sensitive (FET)	$>10^5$	<200	1000	1000	0.3
Common base (bipolar)	4300	1120	1000	1500	0.5
Common base + charge division	1460	1900	1000	2200	0.7

sensitive amplifier (FET-input), (2) common base amplifier (bipolar transistor), and (3) common base amplifiers on both ends of a resistive anode wire (R_a = 2.2 kΩ) for position determination along the wire using charge division.[11]

The common base input stage has the advantage of providing a fast current signal that requires very little further shaping, and it is simple in construction and operation. However, under certain conditions the low equivalent parallel noise resistance produces considerably more noise than occurs in a charge-sensitive amplifier.

For the signal, conservative assumptions are made. After 25 ns, the positive ions have traveled 50 μm, and the fraction of induced charge is 0.20 of the total charge Q_o. Since one is interested in measuring the arrival of the "first electron," only about 1/10 of the total ionization in a 1-cm gap is useful. Therefore, the induced charge to be considered after 25 ns is $Q = 0.02Q_o$. Assuming an appropriate avalanche size of $Q_o = 2\times10^6$ electron charges for the ISABELLE environment and the rise time of the signal to be about twice as fast as the linear approximation, one obtains $ds/dt \approx 3.2 \times10^3$ e ns^{-1}.

Table 2 shows that in all cases the time resolution will be $\ll$1 ns, which corresponds (v_{drift} = 5 cm/μs) to an equivalent position error of $\sigma < 50$ μm. The time resolution is a function of avalanche size and is therefore strongly coupled to considerations of lifetime, saturation effects, rates, etc.

The statistical fluctuations and electron diffusion are clearly dependent on the gas used in the drift chamber and determine the intrinsic spatial resolution of the device. The statistical fluctuations are particularly important near the anode wire, where the resolution is limited by the mean distance between primary clusters. For some drift-chamber geometries, the resolution near the field wires is also reduced by this effect.

In general, farther from the anode wire the dominant effect will be due to electron diffusion. For a drift distance of ~5 mm, this contribution to the spatial resolution is of the order of 50 to 70 μm and is proportional to the square root of the drift distance. For the relatively short drift distances that will be required for the ISABELLE environment, the intrinsic spatial resolutions of drift chambers can be $\lesssim$100 μm. This intrinsic resolution seems to be somewhat larger than the electronic time resolution. However, the numbers quoted for the amplifiers are op-

timum values, which in practice may not be reached, so that one can expect overall spatial resolutions of the order of 100 to 200 μm. For a very large number of channels the circuits certainly will be simpler, and the upper part of the range has to be considered.

Double Pulse Resolution

Multitrack resolution of drift chambers requires the capability of recording the appropriate number of hits per wire in an event and depends on the electronic occupation time of the amplifier-discriminator as well as on the intrinsic time and space resolutions of the chamber itself. Electronically, a double track resolution better than 1.5 mm can be achieved,[12] and systems[13] already exist for recording multiple hits on a single wire with comparable time resolutions.

However, in a drift chamber operated in the proportional mode one cannot distinguish a second avalance unless it arrives after all the clusters from the first track have been collected. This collection time is typically 100 to 200 ns and corresponds to a double track resolution of the order of 5 to 10 mm.

By using relatively thin chambers and perhaps operating at saturating gas gains,[12] one can improve the double track resolution to some degree, especially for tracks incident normally to the anode plane. Double track resolutions of the order of 2 mm (40 ns) have been achieved with this method. Another way to obtain good double track resolution may be simply to reduce the cell size by adding electronegative gas to a multiwire proportional cluster. Including an appropriate number of such proportional and/or drift chambers in the detector would improve the double track resistance of the whole system.

Momentum Resolution and Multiple Scattering

Consider a system of N + 1 parallel drift chambers uniformly spaced in a uniform magnetic field that is parallel to the anode wires. The momentum resolution due to the spatial resolution of the chambers is[14]

$$\left(\frac{\delta p_o}{p_o}\right)^2 = f(N)\left(\frac{p\sigma_x}{BL^2}\right) + g(N)\left(\frac{\tan\lambda}{1+\tan^2\lambda}\,\frac{\sigma_z}{L}\right)^2 \qquad (12)$$

where

p_o = total momentum,
p = component of the momentum normal to the magnetic field,
B = magnetic field strength,
L = distance between the first and last chambers,
λ = complement of the angle between p_o and B,
σ_x = spatial resolution in the dirft direction,

σ_z = spatial resolution along the anode wire,
$f(N) \approx 720/N + 5$ for $N^3 \gg 1$, and
$g(N) \approx 12/N + 3$ for $N^3 \gg 1$.

For 16 chambers at 10-cm intervals (L= 1.5 m) in a 20-kG magnetic field with $\sigma_x = 0.2$ mm, $\sigma_z = 2$ cm, and $\lambda = 45^\circ$,

$$\left(\frac{\delta p_o}{p_o}\right)^2 = \left(\frac{p}{1100\ \text{GeV}}\right)^2 + (0.0054)^2 \ . \tag{13}$$

Note that for particles having momenta $\geq$10 GeV, the momentum resolution is not seriously degraded by a much lower spatial resolution in the magnetic field direction even for tracks at quite large angles relative to the bending plane. This is particularly appropriate to "bicycle-wheel" detectors, where one usually relies on two-dimensional readout methods to measure the coordinate parallel to the anode wires (see below).

For tracks normal to the magnetic field the uncertainty in the momentum measurement due to multiple scattering is approximately

$$\left(\frac{\delta p}{p}\right)_{M.S.} = h(N)\frac{0.015\ \text{GeV}}{\beta BL}\sqrt{\ell/\ell_{rad}} \tag{14}$$

where ℓ/ℓ_{rad} = number of total radiation lengths assumed to be equally distributed, $\beta = v/c \approx 1$, and $h(N) = 1.2$ for large N. For B = 20 kG and L = 1.5 m,

$$(\delta p/p)_{M.S.} = 0.02\sqrt{\ell/\ell_{rad}} \ . \tag{15}$$

Table 3 shows the effect of multiple scattering on momentum resolution for the 16-chamber system considered above for three types of chamber construction. It was assumed that there was air between the chambers.

Table 3

Effect of Multiple Scattering on Momentum Resolution

Material	ℓ/ℓ_{rad}	$(\delta p/p)_{M.S.}$
16 typical chambers (0.001 r.l.)	0.020	0.003
16 foam chambers (0.004 r.l.)	0.065	0.005
16 thin-foil chambers (0.0002 r.l.)	0.009	0.002
1.5 m Ar (1 atm)	0.014	0.002
1.5 m Ar (10 atm)	0.135	0.007
1.5 m Xe (1 atm)	0.100	0.006
1.5 m Xe (10 atm)	1.00	0.020
1.5 m propane (1 atm)	0.0065	0.002
1.5 m propane (3 atm)	0.020	0.003

Also included are the effects of 1.5 m of the gases that have been suggested as being appropriate for dE/dx counters. The propane fillings give results comparable with those for conventional chambers of wire and thin foil construction. The results with Xe and high pressure Ar are somewhat worse but still compatible with those for conventional foil chambers. However 10 atm of Xe is ~1 radiation length and would cause considerably more multiple scattering than that in conventional chambers.

For comparison, we show below the momentum resolution for the 16-chamber system considered above and for the 56- and 448-sample systems that were considered for dE/dx measurements. A chamber resolution of 0.2 mm is assumed.

No. samples in 1.5 m	$(\delta p/p)_{Res.}$ (GeV^{-1})
16	p/1100
56	p/1950
448	p/5350

It is clear, for example, that for a dE/dx chamber containing Xe at 10 atm one does not need 0.2-mm resolution for momentum determination because multiple scattering dominates the momentum resolution for momenta up to ~40 GeV for 56 samples and up to ~100 GeV for 448 samples.

More generally, the effect of multiple scattering on momentum resolution can be seen by considering the conditions and the momentum p^* under which multiple scattering and spatial resolution contribute equally to the momentum determination. Under these conditions (for N + 1 uniformly spaced samples),

$$p^* \approx 6.7\times10^{-4} \frac{L}{\sigma_x} \sqrt{\ell/\ell_{rad}(N + 5)} \quad (GeV/c), \tag{16}$$

and, for L = 1.5 m and σ_x = 200 μm, one obtains

$$p^* \approx 5\sqrt{\ell/\ell_{rad}(N + 5)} \quad (GeV/c) . \tag{17}$$

In summary, it is found that the high number of cells (typically 100) required for dE/dx measurements also have considerable influence on the momentum resolution. A position resolution of $\sigma \approx 200$ μm, which is easily obtained with an avalanche size of $Q_o \approx 2\times10^6$ electrons, already gives excellent momentum resolution. However, the considerable thickness of the pressurized counting gas introduces such strong multiple scattering that it may limit the momentum resolution to <5 GeV/c if high Z noble gases are used.

R.S., A.H.W., C.D.W.

TWO-DIMENSIONAL READOUT

Two-dimensional readout ideally reduces the chamber data to points in three dimensions with good accuracy in all coordinates. These are reconstructed from a constrained triplet of time and/or pulse-height information in the anode wire plane. Here we summarize known methods of 2-D point localization according to spatial accuracy, electronics requirements, and multihit capability.

The last refers specifically to determining the probability of reconstruction of a multihit event. For simplicity we consider first only the reconstruction in space, the time distance between events being large compared with the memory time of the system. The high rate behavior can then be deduced easily by replacing the hit multiplicity of a single event by the apparent hit multiplicity within the memory time, adding random hits.

Delay Lines

The intrinsic resolution given by the noise analysis of Radeka[10] is

$$\frac{\delta \ell}{\ell} = 2.46 \frac{\tau_{FW}}{\tau_D} \frac{e_n}{Z_o Q_o \epsilon} \tau_{FW}^{\frac{1}{2}} \qquad \text{[FWHM]} \tag{18}$$

where

τ_{FW} = time dispersion of the line,
τ_D = total delay time,
e_n = noise voltage/$\sqrt{\text{Hz}}$, and
$Q_s = \epsilon Q_o$ = charge induced on the delay line within the collection time.

For τ_D/τ_{FW}, values ranging from 6 to 14 have been measured.[15-18] We use 10 as a standard value. To obtain the expected resolution from this technique, we set $Z_o = 500\ \Omega$, $e_n = 1\ \text{nV}/\sqrt{\text{Hz}}$, and $\tau_{FW} = 50$ ns, and we assume 100% coupling efficiency. Then

$$\frac{\delta \ell}{\ell} = \frac{1.1 \times 10^{-16}}{\epsilon Q_o}$$

and, for an avalanche size of 2×10^6 electrons with a collected charge in 200 ns of 6×10^5 electrons, one obtains $\delta\ell/\ell = 1 \times 10^{-3}$. Simple helical delay lines have been reported[17] giving results compatible with Eq. (18).

In practice, coupling efficiency is of the order of 30%, but it could be increased by, for example, surrounding the drift cell with the windings of the delay line.[18]

One channel of delay line readout is required per drift cell. Printed circuit delay lines have been used[19] with a sense wire doublet to remove left-right ambiguities with doublet spacings as

small as 6 mm. However, up to now, the spatial resolution is lower than in helical delay lines at the same avalanche size.

The occupation time of an anode pulse, τ_A, gives rise to a dead region in the drift cell. The width is given by $\tau_A V_D$, with V_D being the drift velocity. The length is clearly the length ℓ of the anode wire, and one loses a strip of area $\tau_A V_D \ell$, which is parallel to the anode wire. The dead region corresponding to a delay line pulse of occupation time τ_{DL} is a strip of area $\tau_{DL} V_D \ell$ crossing the dead area of the anode at an angle of $\theta = \tan^{-1}(V_D/V_{DL})$. For a constrained triplet of time measurements, geometry gives the additional dead area incurred by this method, and a fast delay line is clearly preferred. We take $\tau_A = \tau_{DL} = 100$ ns, $\ell = 1.5$ m, and $V_D = 5$ cm/μs. Then one loses an additional 40% at V_{DL} of 1 cm/ns, which increases to 160% for $V_{DL} = 0.1$ cm/ns.

Charge Division

Here the limiting spatial resolution is

$$\frac{\delta \ell}{\ell} = 2.54 \frac{(kTC_D)^{\frac{1}{2}}}{Q_s} \left(\frac{\tau_F}{R_D C_D} \right)^{\frac{1}{2}} \sqrt{2} \qquad \text{[FWHM]} \qquad (19)$$

where Q_s is the signal charge within τ_F, and C_D is the anode wire capacitance. For the anode resistance, R_D, and the shaping time, τ_F, we take the values[11] of 2.2 kΩ and 0.25 μs, respectively, which gives

$$\frac{\delta \ell}{\ell} = \frac{1.46 \times 10^4}{Q_s} \qquad \text{[FWHM]} .$$

This calculation, which implies 1.6% at an avalanche size of $Q_o = 2 \times 10^6$ electrons ($Q_s = 0.45 Q_o$), agrees with the measurements.

In addition to its simplicity of construction, this method clearly lends itself to pulse-height measurement. If this information is not required, unconventional electronics such as dividing analog-to-digital converters could be used.

Left-right ambiguities are not resolved unless one staggers successive wires.[20]

There is, in principle, no loss in multihit capability with this method beyond the loss given by the occupation time of the anode pulse τ_A. Tests with preamplifiers with common base input indicate that pulses can be shaped for high gas gain to ~65 ns.

Cathode Strips

Here, one segments the cathode planes and uses these strips to sample the induced pulses, which are distributed with a full width at half maximum of ~0.5d, with d being the gap width.[21,22] To estimate the noise contribution to the resolution, we assume the

charge to be measured over k strips of width d/2 (for simplicity we consider k even), each with a noise Q_{rms} and obtain

$$\delta\ell = \frac{2.3}{2}\,\frac{Q_{rms}}{Q_s}\,d\sqrt{2\sum_{n=1}^{n=k/2} n^2} \quad . \tag{20}$$

Inducing half the avalanche charge in each cathode plane over four strips (k = 4) and measuring 34% of this within a collection time of 100 ns, we find with $Q_{rms} \approx 4.5\times10^3\ e_o$ (charge-sensitive amplifier gives only about 10% less than the common base input stage) $\delta\ell \approx 0.8$ mm for an avalanche size $Q_o = 2\times10^6\ e_o$.

To evaluate the multihit capability of this scheme, we assume the anode plane to be 1 m^2, composed of 1-m drift cells, and the cathode strips to have angles of $\pm45^o$ with respect to the anode wires. In order to resolve ambiguities, one has three possible alternatives for correlating information: (1) time correlation[21] of cathode planes, (2) amplitude correlation[23] of cathode planes, and (3) measurement of additional coordinate from anode readout.[24]

The time correlation is limited by the signal-to-noise ratio, which can be calculated in the same way as for the anode signal with Eqs. (9), (10), and (11), only the higher capacity ($C_{in} \approx 200$ pF) gives a higher noise. With $Q_{rms} \approx 8\times10^3\ e_o$, and only half the charge as on the anode, $ds/dt = 1.6\times10^3\ e_o$/ns, the time resolution becomes $\delta = 5$ ns. A correlation would be allowed for $\pm3\delta$ which defines a time interval of 30 ns. If the maximum drift time is 100 ns, in about one third of all cases, no correlation can be found. Subdividing the cathode strips into shorter pieces would considerably reduce this number (25-cm-long strips would give only 8% confusion).

For the method of amplitude correlation, physical processes are responsible for its limitation. Naively, one would expect that the two charges induced from the same positive charge at the anode wire are the same on both cathode planes. However, the fluctuation of ionization above and below the anode plane gives different induced charges on the upper and lower cathode because of the top/bottom asymetry of the induced cha s.[22] Measuring an induced pulse on one cathode, one has to allow a variation of 10 to 20% for the corresponding pulse on the other cathode, depending on gas gain and geometry. Since the total possible variation is of the order of 50 to 80% (Landau distribution), this method does not resolve the ambiguity in 25% of the cases.

If the anode wire is used as a third coordinate, the resolving power for ambiguities is given by the total dead area for a single hit, which is

$$A_d = \ell(4d + \tau_A V_D) \ , \tag{21}$$

since the induced pulse is spread over four strips, each d/2 wide. The ratio of the dead area to the total area then gives the

probability for unresolved ambiguities. For $\tau_A V_D \approx d$, one obtains for this ratio 1:20, which gets worse for smaller chambers. This number is also the practical limit for the timing method, for obvious reasons.

Conclusions

For a chamber of 1-m length, ultimately a resolution of about 1 mm can be obtained with delay lines or cathode strips at an avalanche size of 2×10^6 electrons. Charge division under such conditions gives a resolution of about 1.6 cm. Ultimately, the best multihit capability would be obtained by using the charge division method. For the delay line, this is slightly worse (40% additional losses), and for the cathode strip readout this depends strongly on the geometry. For the typical layout chosen, the losses are about a factor of 5 above the value for the current division.

A.H.W., S.W.

PARTICLE IDENTIFICATION USING dE/dx MEASUREMENT

Investigation of the hadronic decay of the hypothetic W or, more generally, investigation of the quark structure of hadrons, requires the recording and analyzing of jetlike events in detail. A particle analyzer of high modularity is needed. Of the two candidates now being discussed, the "imaging Cerenkov counter" and the dE/dx measurement in a multilayer track detector, the latter has the advantage that at least one working system exists,[25] which gives confidence that the systems proposed for ISABELLE (clearly more ambitious) also would be feasible.

The system described by Lehraus et al.[25] samples the energy loss over 5 m of track length, a value considered much too long for a central detector at ISABELLE since it requires a detector of 10-m diameter which has to be surrounded by the magnet coil, shower counters, and μ-identifier. Also, a wide-angle spectrometer[26] would not have enough space for a detector with this dimension. Therefore, in 1977 the question was raised[27] whether sufficient particle resolution can be obtained for an effective track length of 1.3 m by optimizing all possible parameters: pressure, gas mixture, and number of subdivisions. The use of Ar at high pressure (5 to 10 atm) or heavy hydrocarbons at somewhat lower pressure (2 to 3 atm) seemed to be promising. In the meantime, a more detailed study[28] shows that substantial improvement under best conditions can be obtained, but at the price of finer subdivision (greater number of layers), higher total costs (if Xe is used), and reduced dynamic range of the momenta.

Conventional dE/dx

Considering the time schedule of the ISABELLE project, one may call a method "conventional" which is just in the stage of its first successful applications. Such a method is the measurement of the relativistic rise of energy loss by means of subdividing the total

absorber into a number of smaller cells acting as proportional counters, measuring the total charge produced in each cell, and using the mean of the 40% smallest pulses as a final result.

The resolution of such a system can be characterized by the separation of these mean values for two particles (E_π - E_K) (here K/π separation is chosen) in units of the r.m.s. fluctuation σ of the mean value obtained for one particle. Table 4 shows these numbers for a momentum of p = 3.5 GeV/c for a total track length of L = 128.8 cm, a subdivision into n layers, and different typical gas mixtures. Where available, the high momentum behavior is characterized by two numbers. $(p_{max})_R$ is the momentum where the quoted resolution has dropped to 0.707 of the value for p = 3.5 GeV/c. It gives the range relative to the best value. The other number $(p_{max})_A$ gives the momentum where the K and π distributions intersect at half height (σ = 2.3) and gives the absolute range.

For each gas the mean ionization potential $\bar{I}$ and density ρ at 1 atm and 20°C are shown. For higher pressure, the density increases linearly. Table 4 reflects the general behavior[28] of gases that makes it possible to classify them according to mean ionization potential and density. Better resolutions are obtained for high ρ and either high or low $\bar{I}$. Pressure and subdivision dependence is such that finer subdivision has almost no influence at atmospheric pressure but becomes very important at higher pressures.

Table 4

K/π Separation at p = 3.5 GeV/c

Gas	$\bar{I}$ (eV)	ρ (mg/cm^3)	Press. (atm)	n	K/π (σ)	$(p_{max})_R$ (GeV/c)	$(p_{max})_A$ (GeV/c)
C_3H_8	50.3	1.88	1	56	3.5	15	23
			3	56	4.6	13	19
			1	448	4.6	15	31
			3	448	6.8	13	25
0.5 Ar + 0.5 C_2H_6	100.8	1.46	1	56	2.9	(between AR-CH_4 and C_3H_8)	
			10	56	4.4		
			1	448	3.4		
			10	448	6.3		
0.9 Ar + 0.1 CH_4	191.2	1.56	1	56	2.7	30	22
			10	56	3.5	26 ←(7 atm)→	50
			1	448	3.1	30	29
			10	448	5.6	26 ←(7 ")→	67
0.875 Xe + 0.05 C_3H_8 + 0.075 CH_4	501.2	4.94	1	56	2.9	65	47
			10	56	3.8	30 ←(5.5 ")→	40
			1	448	3.4	65	70
			10	448	6.8	30 ←(5.5 ")→	66

Unfortunately, the "best cases" have their special disadvantage, such as restricted momentum range for dense hydrocarbons and high number of subdivisions, high cost, and a considerable total thickness (about 1 radiation length for pressurized Xe). The systematics in the behavior of the gases investigated make it unlikely that a "magic gas" may be found, solving all problems at once.

In addition, the choice of gases working properly in a proportional wire chamber is restricted to a few gases and mixtures thereof, and this is even more true in a drift chamber. The choice of the mixture and cell size depends, therefore, strongly on the experiment. If excellent particle separation is vital, one will consider using high pressure Xe in small subdivisions, using hydrocarbons, or providing more space for the detector. In the first-generation experiment at ISABELLE, it may be sufficient to use an intermediate gas (Ar-C_3H_8, Ar-C_2H_6, Ar-CO_2, or the like) in a detector with fine subdivisions (e.g., 4 mm) but to connect three or four wires together to reduce the number of readout channels. With such an apparatus, a reasonable π/K separation (about 4.5σ at 4 atm) and a K/p determination on a statistical basis (2.6σ) can be obtained. If it turns out to be absolutely necessary, improvement is possible by changing the gas, the pressure, and the number of readout channels.

Unconventional dE/dx

Table 4 shows that for the "conventional" way of measuring dE/dx the improvement in particle separation only can be obtained by increasing the pressure and therefore restricting the dynamic range of momentum.

For a number of physics programs at ISABELLE, however, it may be of importance to separate particles at higher momenta ($p > 30$ GeV/c). A study at Fermilab[29] showed that a combined transition radiation detector plus dE/dx system may be useful to solve this problem. At very low pressure (Xe at about 30 mm Hg) the energy loss in a single cell (4 mm) had much smaller fluctuation, almost no tail as typical for the Landau distribution, and better particle separation than expected from extrapolation of the calculations at higher pressure[28] (see also Table 4). This study showed that in the domain of single clusters the resolution may indeed improve considerably, and it may show the direction for further improvement.

Another approach is being investigated at BNL.[30] It has been frequently observed that a sharply differentiated anode signal shows several subsequent peaks for tracks crossing the chamber in the neighborhood of an anode wire. This structure is attributed to the statistical fluctuations of the primary ionization. Very large peaks may correspond to single δ rays (large cluster). Two possible methods of obtaining a signal for particle identification based on the relativistic rise of the primary ionization are discussed here and compared with the standard method of measuring the total ionization (integrated pulse).

In principle, the number of clusters can be counted (see also Cobb et al.,[31] which would yield a Poisson distribution with a much smaller variance than the distribution of total charge (Landau distribution). Counting all clusters (in Ar at 1 atm one obtains 20 clusters/cm) would give an improvement over the integrating method by a factor of about 2! Unfortunately, this is not possible with present technology. One has to count at least 5 clusters/cm for the aforementioned gas in order to break even with the integrating method, and any improvement is particularly difficult, since the better information is hidden in the small clusters (1 and 2 electrons) as shown by a Monte Carlo calculation.[32] Until now, no serious attempt has been made to understand and improve the fast signal extraction in proportional counters, but it may be rewarding to do so.

Another way of using the time structure of the differentiated signal consists of sampling the pulse height in small time bins (using a multithreshold-multishift register), discarding the big signals, and using the integrated information of the (e.g., 40%) smallest signals. This method represents the state of the art (at least in the ISABELLE time schedule) and gives an improvement over the standard method in the sense that it permits the use of very fine sampling while the number of chamber planes, wires, and amplifiers remains reasonable. An "effective" gap width of about 2 mm (corresponding to 40-ns-wide time slices) seems reasonable, and the data (as in Table 4) can be used to estimate the improvement over the measurement in a 1-cm gap. Depending on gas and pressure, improvement by a factor of 1.2 to 1.7 may be obtained.

Conclusion

The standard technique of measuring the relativistic rise of ionization in gases (total ionization measurement) will give satisfactory results only at higher pressure. Better results can be obtained for lower momenta ($p \leq 15$ GeV/c) or with expensive Xe and a very large number of readout channels (of the order of 10^4). Deeper insight into the ionization process and signal formation may lead to substantial improvement, but further investigations are needed.

H.O., Y.T., A.H.W.

REFERENCES

1. A.H. Walenta, in ISABELLE 1977 Summer Workshop, p. 41, BNL 50721.
2. F.E. Paige, Ibid., p. 202.
3. J. Alspector et al., Ibid., p. 87.
4. A. Etkin, Ibid., p. 40.
5. J. Fischer, S.E. Sobottka, and A.H. Walenta, To be published.
6. H.B. Jensen, Private communication.
7. J. Fischer, H. Okuno, V. Radeka, and A.H. Walenta, To be published.

8. D. Nygren, Private communication.
9. G. Charpak, G. Melchart, G. Petersen, F. Sauli, E. Bourdin, B. Blumenfeld, C. Duchazeaubeneix, A. Garin, S. Majewsky, and R. Walczak, New Approaches to High Rate Particle Detectors, CERN 78-05, 1978.
10. V. Radeka, IEEE Trans. Nucl. Sci. NS-21, 51 (1974).
11. V. Radeka and P. Rehak, IEEE Trans. Nucl. Sci. NS-25, 46 (1978).
12. A. Breskin, G. Charpak, F. Sauli, M. Atkinson, and G. Schultz, Nucl. Instrum. Methods 124, 189 (1975).
13. For a summary see M. Atac and T. Droege, Notes on Drift Chamber Time Digitizer Meeting, Fermilab Report TM-553, 1978.
14. See, e.g., R.L. Gluckstern, Nucl. Instrum. Methods 24, 381 (1963).
15. R. Grove, I. Ko, B. Leskovar, and V. Perez-Mendez, Nucl. Instrum. Methods 99, 381 (1972).
16. CERN-Columbia-Oxford-Rockefeller Collaboration, A system of cylindrical drift chambers in a superconducting solenoid, in Proc. Wire Chamber Conf., Vienna, 1978; Nucl. Instrum. Methods, in press.
17. H. Okuno, R.L. Chase, J. Fischer, and A.H. Walenta, IEEE Trans. Nucl. Sci. NS-24, 213 (1977).
18. O. Achtenberg, A.F. Garfinkel, G. Flügge, H. Jensing, W. Zimmermann, H. Meyer, and M. Rössler, in Proc. Wire Chamber Conf., cf. ref. 16.
19. M. Atac, R. Bosshard, S. Erhan, and P. Schlein, IEEE Trans. Nucl. Sci. NS-24, 195 (1977).
20. J. Heintze, Drift chambers and recent developments, in Proc. Wire Chamber Conf., cf. ref. 16; C.W. Fabjan, J. Lindsay, F. Piuz, F. Rangard, E. Rosso, A. Rudge, S. Serednyakow, W.J. Willis, H.P. Jensen, and J.D. Petersen, Ibid.
21. A.H. Walenta, Thesis, Heidelberg, 1972.
22. J. Fischer, H. Okuno, and A.H. Walenta, Nucl. Instrum. Methods 151, 451 (1978); A.H. Walenta, Ibid., 461.
23. CELLO - Proposal for a 4π Magnetic Detector for Petra, DESY-Karlsruhe-München-Orsay-Paris-Saclay, Fall 1976.
24. G. Fischer and J. Pilchur, Nucl. Instrum. Methods 100, 515 (1972).
25. I. Lehraus, R. Matthewson, W. Tejessy, and M. Aderholz, Nucl. Instrum. Methods 153, 347 (1978).
26. D.H. White, in 1976 ISABELLE Workshops, p. 54, BNL 50611.
27. J. Fischer, H. Okuno, and A.H. Walenta, in ISABELLE 1977 Summer Workshop, p. 90, BNL 50721.
28. J. Fischer, H. Okuno, A.H. Walenta, and C.L. Wang, To be published.
29. A.G. Oganessian, A.T. Sarkissian, and M. Atac, Nucl. Intrum. Methods 145, 251 (1977).
30. E.D. Platner, Private communication.
31. J.H. Cobb, W.W.M. Allison, and J.N. Bunch, Nucl. Instrum. Methods 133, 315 (1976).
32. V.C. Ermilova, L.P. Kotenko, and G.I. Merzon, Nucl. Instrum. Methods 145, 555 (1977).